Kupffer's vesicle is a ciliated organ of asymmetry in the zebrafish embryo that initiates left-right development of the brain, heart and gut

Jeffrey J. Essner*,†, Jeffrey D. Amack*, Molly K. Nyholm‡, Erin B. Harris and H. Joseph Yost§

Huntsman Cancer Institute, Center for Children, Department of Oncological Sciences, University of Utah, Salt Lake City, UT 84112, USA

*These authors contributed equally to this work
†Present address: Discovery Genomics, Minneapolis, MN 55413, USA
‡Present address: University of Wisconsin, Madison, WI 53706, USA
§Author for correspondence (e-mail: joseph.yost@hci.utah.edu)

Accepted 23 December 2004

Development 132, 1247-1260
Published by The Company of Biologists 2005
doi:10.1242/dev.01663

Summary

Monocilia have been proposed to establish the left-right (LR) body axis in vertebrate embryos by creating a directional fluid flow that triggers asymmetric gene expression. In zebrafish, dorsal forerunner cells (DFCs) express a conserved ciliary dynein gene (*left-right dynein-related1*, *lrdr1*) and form a ciliated epithelium inside a fluid-filled organ called Kupffer's vesicle (KV). Here, videomicroscopy demonstrates that cilia inside KV are motile and create a directional fluid flow just prior to the onset of asymmetric gene expression in lateral cells. Laser ablation of DFCs and surgical disruption of KV provide direct evidence that ciliated KV cells are required during early somitogenesis for subsequent LR patterning in the brain, heart and gut. Antisense morpholinos against *lrdr1* disrupt KV fluid flow and perturb LR development. Furthermore, *lrdr1* morpholinos targeted to DFC/KV cells demonstrate that Lrdr1 functions in these ciliated cells to control LR patterning. This provides the first direct evidence, in any vertebrate, that impairing cilia function in derivatives of the dorsal organizer, and not in other cells that express ciliogenic genes, alters LR development. Finally, genetic analysis reveals novel roles for the T-box transcription factor *no tail* and the Nodal signaling pathway as upstream regulators of *lrdr1* expression and KV morphogenesis. We propose that KV is a transient embryonic 'organ of asymmetry' that directs LR development by establishing a directional fluid flow. These results suggest that cilia are an essential component of a conserved mechanism that controls the transition from bilateral symmetry to LR asymmetry in vertebrates.

Key words: Left-right patterning, Cilia, Kupffer's vesicle, Dorsal forerunner cells, Left-right dynein, Organogenesis

Introduction

The external body plan of vertebrates is bilaterally symmetric, but many internal organs, including the heart, digestive organs and parts of the brain, display highly conserved left-right (LR) orientations that are essential for their functions. Members of the *nodal* and *lefty* cell-signaling families and *pitx2*, a *bicoid*-like transcription factor, display similar asymmetric expression patterns in the lateral plate mesoderm in chick, mice, frog and zebrafish embryos (reviewed by Yost, 1999). These genes are also asymmetrically expressed in the zebrafish brain during development (Bisgrove et al., 1999; Essner et al., 2000; Rebagliati et al., 1998; Thisse and Thisse, 1999). Perturbations of these asymmetric gene expression patterns correlate with alterations in brain, heart and gut LR morphogenesis.

A central question in developmental biology is what mechanism initiates asymmetric gene expression and subsequent asymmetric organogenesis? In mice, an elegant model has been proposed in which monocilia protruding from cells in the late gastrula node direct an asymmetric flow of extracellular fluid that results in the establishment of asymmetric gene expression (Nonaka et al., 1998). This 'nodal flow' model is supported by the observations that LR defects are caused by mutations in microtubule motor proteins that affect either ciliogenesis, such as Kif3a (Marszalek et al., 1999; Takeda et al., 1999), Kif3b (Nonaka et al., 1998) and Polaris (Murcia et al., 2000), or cilia motility, such as Left-right dynein (Lrd), which is encoded by the *iv* gene (Supp et al., 1999). The strongest arguments for a role for nodal flow in the establishment of LR asymmetries come from cultured mouse embryos in which externally applied rightward fluid flow can reverse LR development in wild-type embryos and externally applied leftward flow can rescue LR development in mutants that would normally have inverted LR orientation (Nonaka et al., 2002).

The nodal flow model was initially proposed to move a peptide-signaling factor, perhaps a member of the FGF, TGFβ or Hedgehog signaling families. More recently, nodal flow has been proposed to function by asymmetrically activating non-motile mechanosensory cilia on the periphery of the node and initiating an asymmetric Ca^{2+} flux (McGrath et al., 2003) (reviewed by Tabin and Vogan, 2003; Yost, 2003). Nodal flow is the earliest known event in murine LR development.

However, genes implicated in ciliated node cell function are also expressed in non-node cells, and mutations of these genes give rise to a variety of laterality phenotypes and more pleiotropic phenotypes, making it impossible to exclude other mechanisms for LR development during early embryogenesis (for reviews, see Tabin and Vogan, 2003; Wagner and Yost, 2000; Yost, 2003). Furthermore, it is not known whether nodal flow is a murine-specific mechanism. Cilia formation and expression of *lrd* homologues have recently been observed in structures analogous to the node in chick, frog (*Xenopus laevis*) and zebrafish embryos (Essner et al., 2002), but the existence of motile cilia and nodal flow has not been demonstrated in non-murine embryos. Further confounding the issue, there are molecular asymmetries that precede the appearance of *lrd* expression and monocilia in *Xenopus* (Kramer et al., 2002; Kramer and Yost, 2002; Levin et al., 2002) and perhaps in chick (Levin et al., 1995; Stern et al., 1995). This raises the issue of whether ciliated cells in other vertebrate embryos generate fluid flow and have a conserved function for ciliogenesis genes in LR development.

In zebrafish, ciliated cells arise in the tailbud at the end of gastrulation (Essner et al., 2002) in a transient spherical organ called Kupffer's vesicle (KV). KV, first described in 1868 (Kupffer, 1868), is a conserved structure among teleost fishes. Electron microscopy studies in the bait fish *Fundulus heteroclitus* have shown that a single cilium (i.e. monocilium) protrudes from each cell lining KV into the lumen (Brummett and Dumont, 1978). In zebrafish, KV is formed from a group of approximately two-dozen cells, known as dorsal forerunner cells (DFCs), that migrate at the leading edge of the embryonic shield (the zebrafish equivalent of the mouse node) during gastrulation. In contrast to other cells in this region, DFCs do not involute during gastrulation, but remain at the leading edge of epibolic movements. At the end of gastrulation, DFCs migrate deep into the embryo and organize to form KV (Cooper and D'Amico, 1996; D'Amico and Cooper, 1997; Melby et al., 1996). During subsequent somite stages, KV is found ventral to the forming notochord in the tailbud and adjacent to the yolk cell. Although KV was first described well over 100 years ago, it remains unknown whether DFCs and KV are mesodermal or endodermal in origin, and it is unclear what role they play during development, leading to the categorization of KV as an embryonic 'organ of ambiguity' (Warga and Stainier, 2002).

Recently, using a novel technique to knockdown gene expression specifically in DFCs, we reported the first evidence that DFCs and/or KV function in LR patterning (Amack and Yost, 2004). Here, we show that cilia that arise inside KV are motile and generate a consistent counterclockwise fluid flow. A combination of laser ablations, embryological manipulations, analyses of mutants and antisense morpholinos against zebrafish *left-right dynein-related1* (*lrdr1*) injected either into all embryonic cells or specifically targeted to DFCs, demonstrates that ciliated KV cells control LR development of the brain, heart and gut. The presence of motile cilia in zebrafish embryos supports the idea that fluid flow is a conserved LR mechanism used in all vertebrates. In addition, we propose a multi-step genetic pathway in which both the T-box transcription factor *no tail* (*ntl*) and components of the Nodal signaling pathway are necessary, either directly or indirectly, for the expression of *lrdr1* in DFCs and for the morphogenesis of KV. Based on these analyses, we propose that KV is a transient embryonic 'organ of asymmetry' that regulates the earliest known step in LR axis specification in zebrafish. These results comprise the first evidence that ciliated cells function during LR development in a non-murine embryo.

Materials and methods

Maintenance of zebrafish stocks and embryo culture

Danio rerio were maintained at 28.5°C on a 14 hour light/10 hour dark cycle. Wild-type zebrafish stocks were obtained from Ekkwill Breeders (Gibsonton, FL). Stocks carrying sur^{ty686}, sur^{ty768}, cyc^{tf219} and cas^{ta56} mutations were originally produced at the Max-Plank-Institute Fur Entwicklungsbiologie; oep^{m134} at MGH/Harvard; ntl^{b195} at the University of Oregon; and flh^{n1} at Newcastle (UK). Embryos were collected from natural spawnings, cultured and staged as previously described (Westerfield, 1995).

Laser ablations

DFCs were ablated from wild-type embryos between shield and 80% epiboly stages using a VSL-337ND-S Tunable Nitrogen Laser (Laser Science) set to 440 nm. The laser was interfaced to a Leica DMRA compound microscope through a fiber optic cable (Photonic Instruments). Heart laterality was scored in DFC-ablated embryos (and all other embryos in this study) by scoring heart looping as normal, reversed or midline in anesthetized embryos at 2 days post-fertilization.

KV disruptions

Embryonic dissections were carried out on agarose pads using 29 gauge needles on dechorionated embryos. Control embryos were also dechorionated at the same time and kept under similar conditions. All dissections were carried out stereotactically in that both the left and right sides were disrupted. Embryos that showed any disruption of the yolk cell were discarded. Embryos with normal *ntl* staining in the notochord were selected for LR marker analysis.

Antisense depletion of Lrdr1

To isolate the 5′ end of zebrafish *lrdr1*, also referred to as *dynein axonemal heavy chain 11* (Unigene # Dr20984), we performed 5′ RACE (rapid amplification of cDNA ends). *lrdr1* cDNA sequence was compared with a genomic DNA contig in the Sanger Institute genome database (www.ensembl.org) that contained the 5′ end of the zebrafish *lrdr1* gene in order to assign exon and intron boundries for the first seven exons. An updated version of the zebrafish genome from Ensembl includes an annotated fragment of *lrdr1* containing the first 10 exons (Gene ID: ENSDARG00000004221). Antisense morpholino oligonucleotides (MO) directed against the *lrdr1* start codon (*lrdr1*-AUG MO: 5′-GCGGTTCCTGCTCCTCCATCGCGCC-3′), the *lrdr1* exon 2/intron 2 splice site (*lrdr1*E2/I2 MO: 5′-ACTCCAA-GCCCTCACCTCTTATCTA-3′), the start codon of *lefty1* (*lft1* MO: 5′-GGCGCGGACTGAAGTCATCTTTTCA-3′) and a standard negative control MO (5′-CCTCTTACCTCAGTTACAATTTATA-3′) were obtained from Gene-Tools. To knock down gene expression in all cells, MO were injected between the one- and four-cell stages as previously described (Nasevicius and Ekker, 2000). To deliver MO specifically to DFCs, fluorescein-labeled MO were injected into the yolk cell between the 512-cell and 1000-cell stages, and embryos with fluorescent DFCs were selected for analysis, as described (Amack and Yost, 2004). RT-PCR was used to determine the effect of *lrdr1*E2/I2 MO on *lrdr1* mRNA splicing. Total RNA was extracted from embryos using TRIzol Reagent (Invitrogen) and cDNA was synthesized by MMLV-RT primed by random decamers (Ambion Retroscript kit). *lrdr1* cDNA was amplified by 35 cycles of PCR using a forward primer (5′-ACATTCACGCCCTTCAAAAC-3′) in exon 2 and a

reverse primer (5′-ACGTCCTGGATCATTTTTGC-3′) in exon 4. Amplicons were confirmed by DNA sequencing.

In situ hybridization

Antisense RNA probes were transcribed in the presence of digoxigenin-11-UTP or fluorescein-12-UTP (BMB) from linearized DNA templates using the Maxiscript kit (Ambion). Free nucleotides were removed using Bio-Gel P-6 Micro Bio Spin columns (BioRad). cDNA templates used included *ntl* (Schulte-Merker et al., 1994), *pitx2* (Essner et al., 2000), *shh* (Krauss et al., 1993), *lft1* and *lft2* (Bisgrove et al., 1999). Different probes and combinations of probes were used for *lrdr1*: the previously reported *lrdr1* RT-PCR product (Essner et al., 2002), a genomic *Hin*dIII to *Hin*dIII fragment subcloned from a PAC corresponding to a region 5′ to the RT-PCR product, and a 5′ RACE PCR product. All *lrdr1* probes produced similar results individually. In situ hybridizations were performed as previously described (Essner et al., 2000), and in some cases were automated using a Biolane HTI in situ machine (Huller and Huttner AG). Embryos were cleared in 70% glycerol in PBST and photographed with a Leica MZ12 stereoscope using a Dage-MTI DC330 CCD camera.

Immunohistochemistry

Embryos were fixed overnight in 4% paraformaldehyde at 4°C and dehydrated stepwise into methanol for storage at –20°C. After stepwise re-hydration, embryos were blocked for 1 hour in 5% goat serum (Sigma), 2% bovine serum albumin (BSA, Sigma) and 1% DMSO in PBST. Embryos were incubated with an anti-acetylated tubulin antibody (1:400, Sigma) and anti-Ntl antibody (1:100, a gift from D. J. Grunwald) (Schulte-Merker et al., 1992) in blocking solution. After washing embryos in 2% BSA and 1% DMSO in PBST, embryos were incubated with FITC-labeled goat anti-mouse IgG2b antibodies (1:500, Southern Biotech) and Alexa 568-labeled goat anti-rabbit antibodies (1:500, Molecular Probes). After washing, embryos were cleared in Slow Fade (Molecular Probes) and the tail region was removed and mounted. Embryos were imaged using an Olympus Fluoview scanning laser confocal microscope with a 60× objective.

Videomicroscopy of cilia

Live embryos were mounted in 2% methylcellulose in a depression slide and cilia were imaged using a Zeiss Axioskop microscope with a 63× DIC objective. Movies were captured with a Photometrics Coolsnap HQ digital camera and Metamorph imaging software.

Fluorescent bead injections

Embryos were removed from their chorions and mounted in 1% low melt agarose in system water on coverslips. Fluorescent beads (0.5-2 μm) (Polysciences) were pressure injected into KV at the six-somite stage. Embryos were imaged on a Zeiss Axioskop 2 microscope with a 10× Plan Apo objective. Movies were taken with a Nikon Coolpix 995 digital camera and manipulated using QuickTime Pro and Photoshop 7.

Results

lrdr1 expression and motile monocilia suggest the function of dorsal forerunner cells in Kupffer's vesicle is analogous to the mouse ventral node

In mouse, *Lrd* (*Dnahc11* – Mouse Genome Informatics) is an axonemal dynein heavy chain gene that is expressed in ciliated ventral node cells and is required for ciliary function and the generation of nodal flow (Supp et al., 1999). In order to identify the embryonic domains that might have a conserved ciliary function during zebrafish LR development, the expression pattern of the *left-right dynein-related1* (*lrdr1*) gene (Essner et al., 2002) was examined by RNA in situ hybridization at several embryonic stages prior to the onset of LR asymmetric gene expression (Fig. 1A-D). Maternal *lrdr1* mRNA was ubiquitous (see Fig. S1 in the supplementary material) prior to the onset of zygotic transcription (512-cell stage), but by late gastrula stages (70-90% epiboly), expression was restricted to dorsal forerunner cells (DFCs) (Fig. 1A). Double in situ analysis of *lrdr1* and *lefty1* (*lft1*), a marker of dorsal margin and midline cells, was used to confirm that *lrdr1* is expressed exclusively in DFCs at 70-90% epiboly (Fig. 1B) and revealed that *lft1* is not expressed in DFCs as previously reported (Bisgrove et al., 1999) but in cells adjacent to DFCs in the embryonic shield/organizer. Sections through embryos stained for either *lrdr1* (Fig. 1C) or *lft1* (Fig. 1D) confirmed these complementary expression patterns. Neither *lrdr1* nor *lft1* was detected in yolk cells.

Consistent with the fate of the DFCs, *lrdr1* expression was observed in KV (Fig. 1E-G) during early somite stages (SS). *lrdr1* mRNA was also detected in the mesoderm of the tailbud at 8 SS (Fig. 1F), in the notochord and floorplate at the embryonic midline and intermediate mesoderm during the formation of the pronephric ducts at 11 SS (Fig. 1G). Similarly, murine *lrd* is expressed in both node and non-node cells in mouse embryos (Supp et al., 1999). The expression of *lrdr1* in

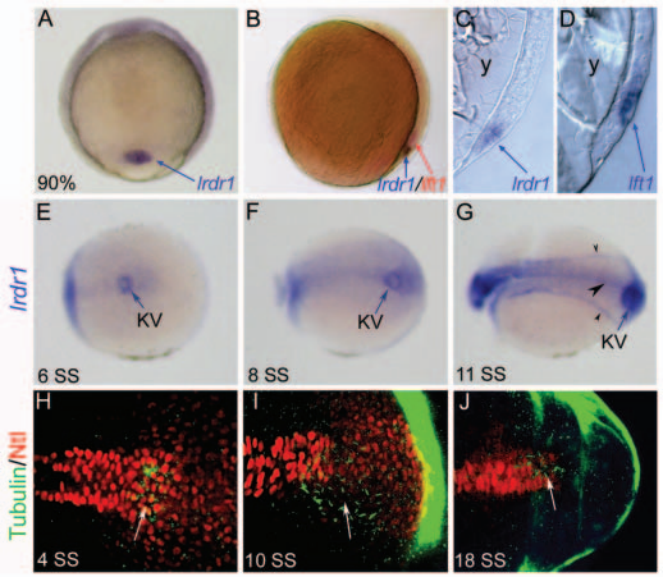

Fig. 1. *lrdr1* is expressed in dorsal forerunner cells (DFCs) and in ciliated Kupffer's vesicle (KV). (A) *lrdr1* is expressed exclusively in DFCs (arrow) at 90% epiboly. Dorsal view, anterior towards the top. (B) Lateral view of an embryo (dorsal on the right) at 80% epiboly stained for *lrdr1* (purple) and *lft1* (red) expression. *lrdr1* is restricted to DFCs, whereas *lft1* is expressed in margin cells and midline cells but not DFCs. Sectioned embryos confirmed that *lrdr1* (C) is expressed in only DFCs and that *lft1* (D) is expressed in cells adjacent to DFCs at 90% epiboly. No expression of *lrdr1* or *lft1* was detected in the yolk (y). (E-G) *lrdr1* RNA expression in KV (arrow) at (E) 6 SS, (F) 8 SS and (G) 11 SS. *lrdr1* was also detected in the tailbud at 8 SS (F) and in the floor plate, notochord and intermediate mesoderm (arrowheads) by 11 SS (G). Posterior-dorsal views with the anterior to the left. (H-J) Immunofluorescence at (H) 4 SS, (I) 10 SS and (J) 18 SS using anti-acetylated Tubulin antibodies (green) to detect cilia and anti-Ntl antibodies (red) to label nuclei in the notochord and KV. Arrows indicate cilia in KV. Embryos were transversely bisected for visualization of the tailbud.

DFCs and KV suggests that these tissues could have an analogous role to the ventral mouse node during LR development.

The progeny of DFCs in KV assemble cilia similar to those observed at the mouse node (Essner et al., 2002). To examine the developmental timing of cilia formation in DFC/KV, we used anti-acetylated Tubulin antibodies to label cilia at different stages during gastrulation and somitogenesis. To aid in the identification of DFCs and KV in whole embryos, anti-Ntl antibodies were used to label nuclei in the notochord, mesoderm and DFCs during gastrulation and in the notochord, tailbud and KV during somitogenesis. Cilia were not observed in the DFC domain during gastrulation (data not shown) but were detected at 4 SS in Ntl-positive cells under the notochord, in the region of KV (Fig. 1H). These cilia initially appeared as short projections into the lumen of the forming KV. Cilia in the well-formed KV were elongated at 10 SS (Fig. 1I) and remained elongated at 15 SS (data not shown). At 18 SS, the lumen of the KV was smaller or absent, although some of the dispersed KV cells remained ciliated (Fig. 1J). Confocal analyses of embryos at 6-8 SS (n=5) revealed a 1:1 ratio between the number of cilia visualized with the anti-acetylated tubulin antibody and the number of nuclei staining positive for Ntl in KV, suggesting KV cilia are monocilia.

To determine whether KV cilia are motile, we used videomicroscopy to examine KV in living embryos. At 6-10 SS, cilia were motile in the lumen of KV (see Movie 1 in the supplementary material). To test whether these cilia are capable of generating fluid flow inside KV, fluorescent beads were injected into KV at the 6 SS. These beads revealed a consistent directional counterclockwise flow inside KV (see Movie 2 in the supplementary material). Flow persisted until 10-12 SS, when asymmetric expression of the Nodal-related gene *southpaw* begins in left lateral plate mesoderm cells at the anterioposterior level of KV (Long et al., 2003). These observations suggested that cilia in KV might function in a manner analogous to cilia in the mouse node during LR development.

Ablation of DFCs alters LR development without other effects on embryogenesis

Murine genes implicated in nodal flow are also expressed in non-ciliated cells, and mutations in these genes, which result in a diverse array of laterality phenotypes and pleiotropic defects in other tissues, do not provide direct evidence that ciliated cells have a role in LR patterning. To directly test whether ciliated cells are required for LR patterning, DFCs were ablated from wild-type zebrafish embryos during gastrulation using a nitrogen laser. To verify that the ablation technique was efficient, embryos were fixed following ablation at 60% epiboly, and stained for *ntl* expression (Fig. 2B) or *lrdr1* expression (data not shown). With this laser-ablation technique, each cell is individually ablated at a specified focal plane, so it is unlikely that underlying yolk nuclei or adjacent mesoderm cells are affected. Ablated embryos lacked *ntl* (n=8/8) and *lrdr1* (n=7/8) gene expression in the DFCs, but had wild-type expression of *ntl* in adjacent mesoderm cells (Fig. 2B). Control embryos displayed wild-type *ntl* expression in both the mesoderm and DFCs (n=5/5, Fig. 2A). These controls indicate that laser ablation provides an efficient approach to eliminate DFCs during gastrulation without altering gene expression in neighboring cells. To examine the effects of DFC ablation on KV formation, DFC-ablated and unablated control embryos were immunostained at 6 SS with anti-Ntl and anti-acetylated Tubulin antibodies (Fig. 2C,D). Although two out of six DFC-ablated embryos had a ciliated KV that appeared similar to control embryos (Fig. 2C), two out of six of the DFC-ablated embryos formed a dismorphic KV that was misshapen (data not shown) and two out of six of the embryos did not form KV (Fig. 2D). These results indicate that ablation can result in a range of effects on KV morphogenesis, which probably reflects the efficacy of DFC ablation.

As the embryonic midline has been shown to be essential for LR development in frogs (Danos and Yost, 1995), zebrafish (Chen et al., 1997; Danos and Yost, 1996) and mice (Meno et al., 1998; Yamamoto et al., 2003), we assessed whether DFC-ablated embryos had intact midline structures. Immediately after ablation, *ntl* expression was normal in adjacent prospective midline cells (Fig. 2B). At 6 SS, the notochord and floorplate were intact as detected by DIC microscopy (data not shown) and Ntl expression was normal in notochord nuclei (n=6/6, Fig. 2D). At 22 SS (Fig. 2E,F), the notochord and floorplate were intact and contiguous, as detected by DIC microscopy (data not shown), and *ntl* and *lft1* expression in DFC-ablated embryos (n=16/17), similar to wild-type embryos (n=71/71). Another indication of intact midline is the specific expression patterns of downstream LR gene expression patterns. Disruption of notochord development results predominantly in bilateral expression of these LR markers in lateral plate mesoderm, as exemplified in *ntl* and *flh* mutants in zebrafish (Bisgrove et al., 1999; Bisgrove et al., 2000) and notochord surgical disruptions in *Xenopus* (Lohr et al., 1997). By contrast, DFC-ablated embryos, displayed relatively low rate of bilateral expression, concurring with the conclusion that midline formation is unperturbed by DFC ablation.

In contrast to normal anterioposterior and dorsoventral development, ablation of DFCs at 60-80% epiboly had significant effects on brain and heart LR development as assessed by the molecular markers *lefty1* (*lft1*) and *lefty2* (*lft2*). *lft1* and *lft2* are normally expressed in the left dorsal diencephalon and left heart field, respectively (Fig. 2G,I). In the diencephalon, DFC-ablated embryos showed equal numbers of embryos with right-sided (35%, Fig. 2H) or absent *lft1* expression (35%) and a few with bilateral or left-sided expression (Fig. 2K). Unablated controls showed wild-type expression of *lft1* (89%, Fig. 2G,K). In the heart field, the majority (53%) of DFC-ablated embryos had inverted expression of *lft2* (Fig. 2J,L). Taken together, our analyses revealed that 82% of DFC-ablated embryos had laterality defects (Fig. 2M), whereas only 11% of unablated control embryos had a laterality marker defect (n=71, data not shown). When heart loop orientation was scored, DFC ablation at 60-70% epiboly resulted in 24% reversed hearts (n=46) and DFC ablation at 70-80% epiboly resulted in 29% reversed hearts (n=14), with control, non-ablated siblings having 2-3% heart reversals (n=274).

Kupffer's vesicle is an embryonic organ of asymmetry

The results from laser ablations of DFCs indicate that DFCs or KV cells are essential for normal LR patterning, but do not define the developmental stages at which this patterning

occurs. To directly test the role of KV in the generation of laterality, KV was disrupted by microsurgery at distinct stages during somitogenesis. The efficacy of KV disruption was analyzed by immunostaining with anti-Ntl and Tubulin antibodies. In control embryos, cilia and KV cells were organized in a normal spherical pattern (Fig. 3C), whereas in KV disrupted embryos this morphology was severely perturbed (Fig. 3D,E, *n*=13/17). In embryos in which KV was disrupted between the 3-7 SS, notochord (assessed by *ntl* expression) and tail development was normal, but expression of the left-side markers *pitx2* in the dorsal diencephalon and lateral plate and *lft2* in heart primordia was altered (Fig. 3G,H,J). By contrast, when the KV disruptions were carried out at 13-15 SS, asymmetric expression of *pitx2* and *lft2* was normal (Fig. 3K). Consistent with the asymmetric gene expression data, heart laterality was reversed in 35% of embryos in which KV was disrupted at 3-7 SS (*n*=23), while KV disruptions at 10-15 SS resulted in a low rate of heart laterality disturbances (4%, *n*=45). Although these results do not exclude the possibility that DFCs play an earlier and separate role in LR development (i.e. during gastrulation) before giving rise to KV, they indicate that KV is a necessary organ for LR patterning at 3-7 SS but is dispensable after 10 SS.

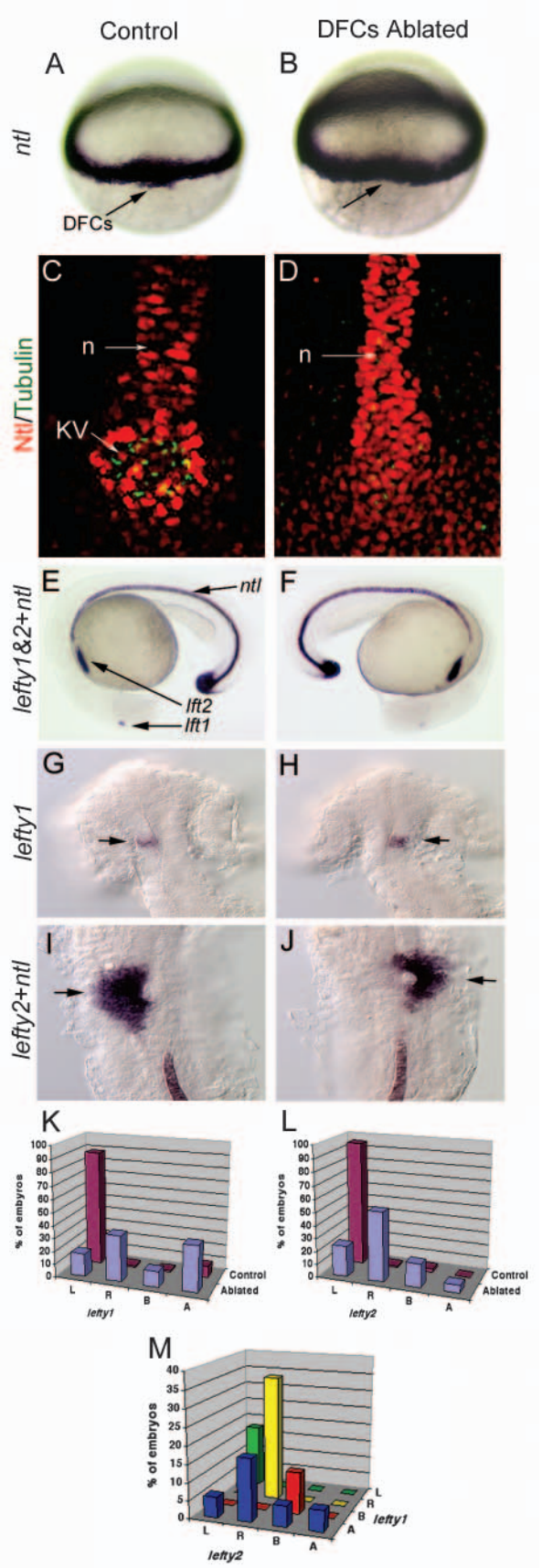

Fig. 2. Laser ablation of DFCs alters LR patterning without affecting development of the midline. Unablated control embryos expressed *ntl* in DFCs (arrow) at 60% epiboly (A) and in the notochord at 24 hours post-fertilization (E). Laser ablation eliminated DFCs (arrow, dorsal view at 60% epiboly) but did not alter *ntl* expression in equatorial mesoderm (B) or in notochord and tailbud at 24 hpf (F). Control embryos (C) and DFC-ablated embryos (D) were immunostained with anti-acetylated Tubulin antibodies (green) to detect cilia and anti-Ntl antibodies (red) to detect the notochord (n) and Kupffers vesicle (KV). Both control and DFC-ablated embryos showed contiguous Ntl staining in the notochord, even in embryos (*n*=2/6) that failed to form KV (D). (G-J) In control embryos, we observed normal expression of *lft1* (arrow) in the left dorsal diencephelon (G) and *lft2* (arrow) in the left heart primordia (I). In DFC-ablated embryos, *lft1* (arrow) in the diencephalon (H) and *lft2* (arrow) in the heart primordia (J) were frequently reversed. (K-M) Analysis of *lft1* expression in the diencephalon (K) and *lft2* expression in the heart primordia (L) in control (*n*=71) and DFC-ablated (*n*=17) embryos. (M) Analysis of *lft1* expression plotted against *lft2* expression in DFC-ablated embryos indicated that the predominant class of DFC-ablated embryos displayed reversal of both brain and heart markers (yellow bar). L, left; R, right; B, bilateral; A, absent gene expression.

lrdr1 expression is required for normal LR development

Mutations in the *lrd* gene in mice result in indeterminate LR patterning. Although there is significant variation among the three mutant alleles (lrd^{lgl}, lrd^{iv}, $lrd^{\Delta P1}$), *lrd* mutant homozygotes display a range of organ laterality defects, from normal situs in ~50% of the mutants, to discordant, randomized organ orientations, to ~40% showing a complete organ reversal (Brown et al., 1989; Supp et al., 1999; Supp et al., 1997). To assess the roles of *lrdr1* in zebrafish, antisense morpholino oligonucleotides (MO) directed against the start codon (*lrdr1*-AUG MO) of the *lrdr1* mRNA were injected into embryos to block translation and deplete Lrdr1 protein. Embryos injected with 2-4 ng of MO at the one- to four-cell stages developed severe axial defects and many died by 2 days postfertilization (dpf). Injecting a lower dose (1 ng) resulted in apparently normal gross development (Fig. 4B), including an intact

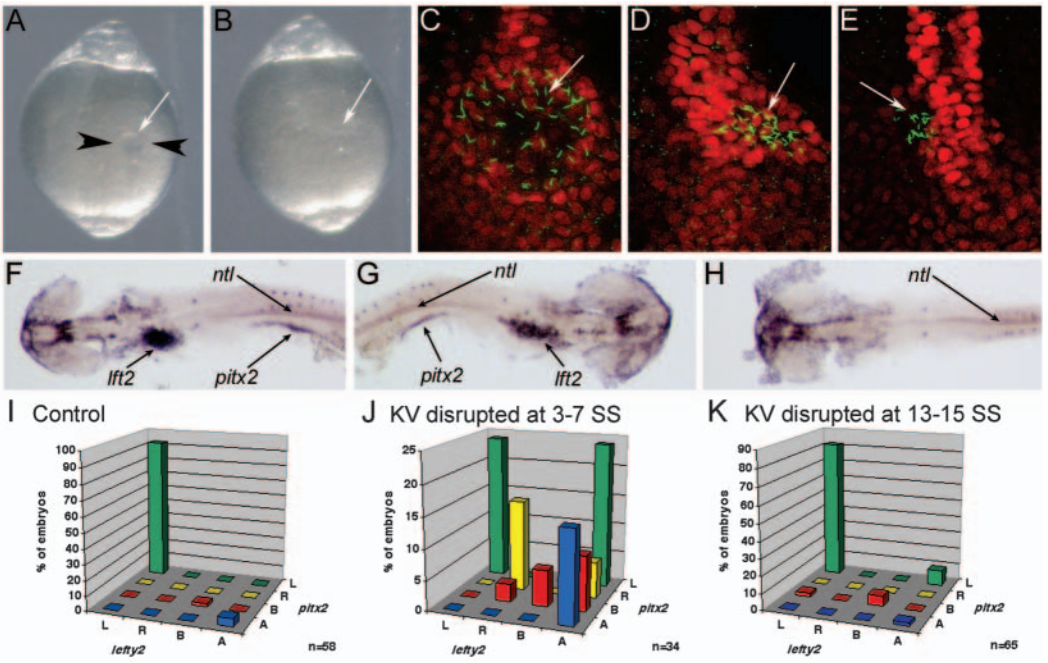

Fig. 3. KV is essential for LR development during early somitogenesis. (A) Image of a live 6 SS embryo prior to disruption of KV. Black arrowheads represent the path of the needles during KV disruption and the white arrow indicates KV. (B) Image of the same embryo in A after disruption of KV. White arrow indicates where KV was previously located. (A,B) Dorsal views of the tail. (C-E) Control embryo (C) and KV disrupted embryos (D,E) stained with anti-acetylated tubulin (green) and Ntl (red) antibodies at 10 SS. Arrows indicate KV cilia. (F-H) In situ hybridization analysis of *lft2*, *pitx2* and *ntl* at 20-25 SS. (F) A control embryo showing normal left-lateral gene expression. KV disrupted embryos often showed either reversed (G) or an absence (H) of lateral gene expression. Arrows indicate *lft2* staining in the heart primordia, *pitx2* staining in the lateral mesoderm and *ntl* staining in the notochord. Yolk was dissected away for visualization of lateral staining. (F-H) Dorsal views with the anterior towards the left in F,H and to the right in G. (I-K) *lft2* expression in the heart primordia plotted against *pitx2* expression in the lateral plate mesoderm in control (I), KV-disrupted at 3-7 SS (J) and KV-disrupted at 13-15 SS (K) embryos. L, left; R, right; B, bilateral; A, absent. *n*, number of embryos examined.

midline, as assessed by expression of *ntl* in the notochord (*n*=66/73, Fig. 4E) and *sonic hedgehog* (*shh*) in the notochord and floor plate (*n*=26/27, data not shown) at 22-26 SS. In addition, KV morphogenesis was normal in MO injected embryos (*n*=78/92) similar to controls (*n*=88/100). Cilia in KV (Fig. 4H) also appeared normal in injected embryos (*n*=10/13) as compared with controls (*n*=14/16, Fig. 4G). However, *lrdr1*-AUG MO-injected embryos had an increased frequency of reversed heart looping (26%, *n*=61), indicating LR patterning was perturbed. Expression of *lft2* in the heart field and *lft1* in the diencephalon was also disrupted in these embryos (Fig. 4E, Table 1). *lft1* often displayed a higher incidence of absence in both MO injected and control embryos, probably owing to variations in the timing of expression. The analysis of *lft1* reveals a previously unrecognized role for Lrd in the regulation of brain asymmetry and taken together with the *lft2* analysis suggests that Lrd plays an evolutionarily conserved role in LR patterning.

The large size of *lrd* mRNAs (>14 kb) precludes conventional rescue experiments in which MO-induced phenotypes are corrected by co-injection of synthetic rescuing mRNA. As an alternative approach to test the specificity of *lrdr1*-AUG MO, we injected a distinct MO that targeted the splice donor site at the junction of exon 2 and intron 2 (*lrdr1*E2/I2 MO). Splice site-blocking MO have been used successfully to disrupt splicing of specific transcripts in zebrafish embryos and, advantageously, the efficacy of splice site-blocking MOs can be measured by RT-PCR (Draper et al., 2001). Using primers in exons 2 and 4 of *lrdr1*, RT-PCR analysis of total RNA extracted from embryos at 2 dpf indicated that injecting *lrdr1*E2/I2 MO blocked the removal of intron 2 from *lrdr1* transcripts and reduced the levels of correctly spliced *lrdr1* mRNA in a dose-dependent manner (data not shown). The retention of intron 2 (confirmed by sequencing RT-PCR products, data not shown) introduces several stop codons in the *lrdr1*-coding sequence. Embryos injected with *lrdr1*E2/I2 MO had phenotypes similar to embryos injected with *lrdr1*-AUG MO. *lrdr1*E2/I2 MO (1.6 ng) injected at the one- to four-cell stages blocked splicing of *lrdr1* mRNA in DFCs at 80% epiboly (Fig. 4J, lane 5), reversed heart looping in 27% of injected embryos (*n*=44) [when compared with 0% in uninjected embryos (*n*=31)], and disrupted expression of LR markers (Table 1). In *lrdr1*E2/I2 MO injected embryos, midline expression of *ntl* (*n*=22/23) and *shh* (*n*=45/46) was intact at 24-26 SS. Furthermore, KV appeared normal in live embryos (*n*=146/162) relative to controls (*n*=58/62) and anti-Tubulin antibodies detected KV cilia at 6-10 SS (*n*=5). In general, *lrdr1*E2/I2 MO had a weaker effect on LR development than did the translation-blocking *lrdr1*-AUG MO (Table 1). This could reflect a difference in the effectiveness of the two MOs or may be due to the presence of maternal *lrdr1* transcripts, which are presumably already spliced before MO delivery and therefore not targeted by *lrdr1*E2/I2 MO. Either of these possibilities would be consistent with the low level of normally spliced *lrdr1* mRNA that remains in *lrdr1*E2/I2 MO embryos (Fig. 6J, lane 5). Although *lrdr1*E2/I2 MO injections resulted in a less penetrant phenotype, the effects on LR patterning corroborate the *lrdr1*-AUG MO data and together show that *lrdr1* is an essential gene for LR development in zebrafish.

lrdr1 expression in DFCs is required for normal LR development

In the mouse embryo, it is not known whether Lrd controls LR development through its expression in ciliated cells in the node

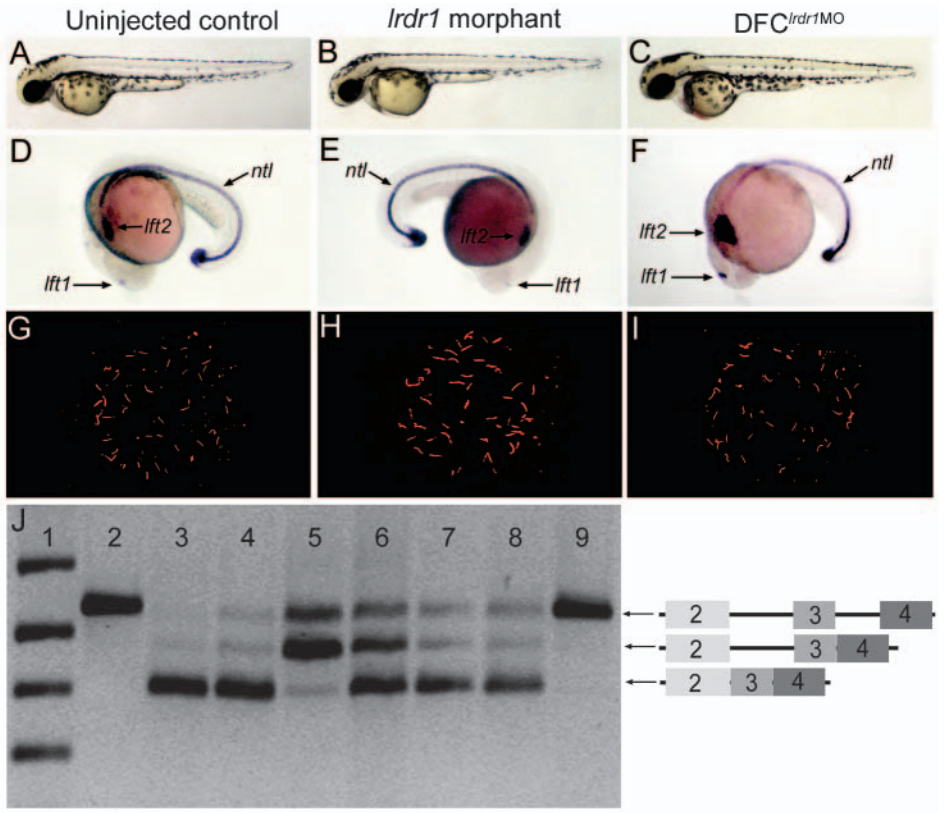

Fig. 4. Morpholino knockdown of *lrdr1* in all embryonic cells or specifically in DFCs perturbs LR patterning without affecting midline or KV development. (A-C) The majority of embryos injected with either 1 ng *lrdr1*-AUG MO (B) or 1.6 ng *lrdr1*E2/I2 MO (not shown) at the one- to four-cell stages (*lrdr1* morphants) and embryos in which 1 ng *lrdr1*-AUG MO + 1.6 ng *lrdr1*E2/I2 MO was co-injected into the yolk at mid-blastula stages to target DFCs (DFC^{lrdr1MO} embryos) (C) appeared similar to uninjected controls (A) at 2 dpf. (D-F) *ntl* expression in the notochord was normal in *lrdr1* morphants (E) and DFC^{lrdr1MO} embryos (F), but expression of the normally left-sided markers *lft1* and *lft2* (D) was altered, including right-sided (E) and bilateral (F) expression. (G-H) KV cilia were detected by anti-Tubulin antibodies (red) in both *lrdr1* morphants (H) and DFC^{lrdr1MO} embryos (I), and resembled cilia in wild-type controls (G). (J) RT-PCR analysis of RNA extracted from embryos between 80-90% epiboly was used to determine the efficacy of *lrdr1*E2/I2 MO in DFCs. Primers in *lrdr1* exons 2 and 4 amplified a fragment of the gene that includes exons 2-4 and introns 2-3 from genomic DNA (lane 2). The predominant cDNA fragment amplified in uninjected embryos (lane 3) and embryos injected with 1 ng of control MO at the one- to four-cell stages (lane 4) corresponds to spliced *lrdr1* mRNA (exons 2-4). *lrdr1*E2/I2 MO (1.6 ng) injected at the one- to four-cell stages (lane 5) or at mid-blastula stage (lane 6) resulted in the accumulation of *lrdr1* transcripts that retain intron 2. This was not observed in embryos injected with *lrdr1*E2/I2 MO between dome stage and 30% epiboly (lane 7) or with 1.5 ng *lft1* MO at mid-blastula stages (lane 8). Negative control reactions that lacked reverse transcriptase (lane 9) amplified only a genomic fragment that probably reflects genomic DNA contamination in RNA extracts. DNA ladder was loaded in lane 1. Diagrams on the right represent the amplicons confirmed by direct sequencing of RT-PCR products.

Table 1. Analysis of *lefty2* and *lefty1* expression in morpholino (MO) injected embryos

			lefty2 (heart field)				*lefty1* (brain)			
Injection stage	Morpholino	*n*	Left	Right	Bilateral	Absent	Left	Right	Bilateral	Absent
	Uninjected	759	91%	3%	5%	2%	77%	2%	8%	13%
One- to four-cell	1 ng control MO	222	88%	6%	4%	2%	59%	4%	4%	33%
	1 ng *lrdr1*-AUG MO	482	50%	32%	6%	13%	34%	20%	2%	44%
	1.6 ng *lrdr1*E2/I2 MO	145	60%	14%	21%	6%	46%	11%	13%	18%
512-1000 cell	1.5 ng *lft1* MO + 2 ng control MO	76	82%	3%	13%	3%	71%	3%	21%	5%
	1 ng *lrdr1*-AUG MO	280	65%	14%	17%	4%	58%	12%	19%	12%
	1.6 ng *lrdr1*E2/I2 MO	99	84%	4%	9%	3%	74%	2%	15%	9%
	1 ng *lrdr1*-AUG MO + 1.6 ng *lrdr1*E2/I2 MO	96	55%	17%	23%	5%	42%	15%	19%	25%
Dome-30% epiboly	1 ng *lrdr1*-AUG MO + 1.6-2 ng *lrdr1*E2/I2 MO	127	87%	3%	9%	2%	76%	2%	9%	13%

MO were injected at the one- to four-cell stages to target all cells, at the 512-1000 cell stages to target DFCs (and the yolk cell) and at the dome-30% epiboly stages to target the yolk cell only. Expression of *lefty2* and *lefty1*, analyzed by in situ hybridization at 22-26 SS, was scored as left-sided, right-sided, bilateral or absent. The percentage of embryos given for each class reflects data pooled from at least three experiments. *n*=number of embryos analyzed.

or through its expression in non-node cells. To test the role of *lrdr1* specifically in KV in zebrafish, we used a recently developed technique to knockdown targeted gene function specifically in DFCs and KV cells (Amack and Yost, 2004). MO injected into 1- to 4-cell embryos knocks down gene function in all embryonic cells (Nasevicius and Ekker, 2000). By contrast, MO injected into the yolk cell at mid-blastula stages (between the 512-cell and 1000-cell stages) diffuses throughout the yolk and, in a subset of embryos, localizes in DFCs. This creates chimeric embryos in which the targeted gene function is knocked down in DFCs but not in other embryonic cells (Amack and Yost, 2004). Fluorescein-tagged

MO allowed fluorescence microscopy to be used to select embryos in which MO had loaded specifically into DFCs and KV. Injecting either 1 ng *lrdr1*-AUG MO or 1.6 ng *lrdr1*E2/I2 MO into the yolk at mid-blastula stages had a weak or no effect on LR development (Table 1). This may be due to inefficiencies of DFC-targeted injections, such as variability in the amount of MO that enters DFCs from the yolk and MO not entering all DFCs in a given embryo (see discussion), or to the presence of maternal mRNA or protein as discussed above. Consistent with these possibilities, RT-PCR analysis showed that although 1.6 ng of *lrdr1*E2/I2 MO injected at mid-blastula stages interfered with *lrdr1* splicing in DFCs at 90% epiboly, this effect was reduced relative to injections at the one- to four-cell stages (Fig. 4J, lane 6 versus lane 5). To increase MO efficacy, 1 ng of *lrdr1*-AUG MO and 1.6 ng of *lrdr1*E2/I2 MO were co-injected into the yolk at mid-blastula stages. In four out of five experiments, co-injected embryos (referred to as DFC$^{lrdr1\text{MO}}$ embryos) showed an increase in aberrant *lft1* and *lft2* LR marker expression (Table 1). In one experiment, however, 93% of DFC$^{lrdr1\text{MO}}$ embryos had normal *lft2* expression (data not shown), further highlighting the variability of DFC-targeting injections and/or MO efficacy. DFC$^{lrdr1\text{MO}}$ embryos that showed LR defects appeared similar to control embryos at 2 dpf (Fig. 4C). Furthermore, DFC$^{lrdr1\text{MO}}$ embryos had intact expression of *shh* (n=91/95) in the midline at the 24-26 SS, developed a normal KV (n=51/71) similar to controls (n=67/89) and formed KV cilia detected by anti-Tubulin antibody staining (Fig. 4I, n=4). These experiments suggest that *lrdr1* plays a role in DFC/KV cells that is important for normal LR development, but do not exclude the possibility of additional roles for *lrdr1* during LR patterning in other embryonic cells and/or the yolk cell.

Controls for DFC^{MO} targeting experiments

Two controls were designed to test whether LR defects caused by injecting *lrdr1* MO at mid-blastula stages were specific to *lrdr1* knockdown in DFCs and their progeny. First, we used MO against *lft1*, which is expressed in adjacent shield cells but not in DFCs during gastrulation (Fig. 1B-D). Consistent with a previous report (Feldman et al., 2002), 1.5 ng *lft1* MO co-injected with 2 ng of fluorescein-tagged negative control MO at the one- to four-cell stages affected the midline and resulted in bilateral expression of *lft1* in the brain (n=27/28) and *lft2* in the heart field (n=28/28). Injecting *lft1* MO + control MO into the yolk at mid-blastula stages resulted in predominantly normal *lft1* and *lft2* asymmetric expression (Table 1). This indicates that MO injected into the yolk at mid-blastula stages do not affect non-DFC cells (e.g. neighboring midline cells) and do not have non-specific effects on LR development. Second, to test whether *lrdr1* MO must enter DFCs to affect LR development, we co-injected 1 ng of *lrdr1*-AUG MO and 1.6-2.5 ng of *lrdr1*E2/I2 MO into the yolk at late blastula stages (dome stage to 30% epiboly), when connections between the yolk and DFCs are thought to be closed (Cooper and D'Amico, 1996). In these embryos, MO diffused throughout the yolk but did not accumulate in DFCs, did not affect splicing of *lrdr1* RNA, which is expressed only in DFCs at 90% epiboly (Fig. 4J, lane 7), and did not disrupt asymmetric expression of *lft1* or *lft2* (Table 1). Although this control does not exclude the possibility that yolk syncitial layer (YSL) nuclei underlying DFCs (D'Amico and Cooper, 2001; Kimmel and Law, 1985) might have a role in LR development, it indicates that if *lrdr1* is expressed in yolk cells, it does not have a detectable role in LR development. Together, these results indicate that *lrdr1* expression in DFCs, which proceed to make ciliated cells in the KV, is essential for normal LR development of the viscera and brain.

lrdr1 is required for fluid flow in KV

Loss of Lrd in mutant mice renders nodal cilia immotile (Supp et al., 1999). To determine if MO knockdown of zebrafish *lrdr1* affected cilia motility and fluid flow in KV, fluorescent beads were injected into KV of *lrdr1*-AUG MO injected embryos. KV appeared normal in these embryos, but flow of fluorescent beads was reduced or absent (Table 2 and see Movie 3 in the supplementary material). Embryos injected with negative control MO showed the characteristic counterclockwise flow seen in wild-type embryos (Table 2). Importantly, *lrdr1*-AUG MO injected embryos from these experiments that were not injected with fluorescent beads showed a high rate (24%, n=58) of heart laterality reversal, whereas all embryos injected with negative control MO (n=61) had normal heart laterality. This indicates that, as in mouse, *lrdr1* is required for cilia motility and provides evidence that fluid flow inside KV is required for zebrafish LR determination.

ntl, *spt*, *oep* and *cas* control distinct steps upstream of *lrdr1* expression and KV organogenesis

DFCs express *lrdr1* and give rise to a ciliated KV that we have shown is essential for the earliest known step in zebrafish LR development. In order to discover genetic pathways that are upstream of this first step, we screened a collection of laterality mutants in zebrafish by five criteria: (1) formation of DFCs; (2) endocytic activity in DFCs; (3) *ntl*, *squint* (*sqt*) and *lrdr1* gene expression in DFCs; (4) organogenesis of KV; and (5) ciliogenesis in KV. As in mouse mutants (reviewed by Wagner and Yost, 2000), the laterality phenotypes of these zebrafish mutants are different, suggesting either pleiotropic phenotypes or disruption of distinct steps in LR patterning. Although the relatively late developmental effects on asymmetric lateral plate markers and organ orientation have been described (Bisgrove et al., 2000; Chen et al., 1997; Chin et al., 2000; Concha et al., 2000; Danos and Yost, 1996; Gamse et al., 2003; Long et al., 2003), the embryonic site of action and primary cause of the laterality defects in each of these mutants remain unknown.

Zebrafish laterality mutants have been classified based on the disruption of the normally left-sided markers *lft1*, *lft2* and *pitx2* (Bisgrove et al., 2000; Bisgrove et al., 2003). In the present study, we examined the following laterality mutants:

Table 2. *lrdr1* MO reduced or abolished fluid flow inside Kupffer's vesicle.

	Strong flow	Reduced flow	Absent flow	*n*
Control MO	7	3	0	10
lrdr1 MO	0	4	6	10

Videomicroscopy was used to capture movies of fluorescent beads successfully injected into KV of embryos injected with either control MO (n=10) or *lrdr1*-AUG MO (n=10) at the one- to four-cell stages. Movies were analyzed in a double-blind fashion and flow of beads inside KV was scored as strong, reduced or absent.

Table 3. Zebrafish laterality mutants have distinct phenotypes in dorsal forerunner cell gene expression and Kupffer's vesicle organogenesis

Mutant	DFC SYTO-11 staining	DFC *ntl* staining	DFC *sqt* staining	DFC *lrdr1* staining	KV organogenesis	KV ciliogenesis
ntl^{b195}	+ (*N*=5)	+*	+ (*n*=30/30)	– (*n*=163/210)	– (*n*=156/203)	+ (*N*=5)
flh^{nl}	+ (*N*=2)	+ (*n*=69/74)	+ (*n*=170/170)	+ (*n*=183/187)	+†	nd
spt^{b104}	+ (*N*=7)	nd	nd	+ (*n*=68/68)	– (*n*=35/50)	+ (*N*=5)
oep^{m134}	+ (*N*=8)	+ (*n*=31/33)	– (*n*=152/186)	– (*n*=85/112)	– (*n*=33/50)	– (*N*=4)
cas^{ta56}	– (*N*=4)	– (*n*=21/26)	– (*n*=20/28)	– (*n*=131/185)	– (*n*=40/59)	– (*N*=5)

Live embryos exposed to SYTO-11 were examined at shield stage for DFC labeling, and mutants were subsequently identified by phenotype at 24 hpf. Expression of *ntl* and *sqt* was observed by in situ hybridization at 60% epiboly and *lrdr1* expression was examined at 90% epiboly. KV formation was examined at 5-12 SS in both living embryos and in fixed embryos by staining with anti-Ntl antibodies. Cilia were observed by staining with an anti-acetylated tubulin antibody in embryos simultaneously probed with anti-Ntl antibodies to identify *ntl*, *spt*, *oep* and *cas* mutants that have KV defects.

+Wild-type; –, absent or reduced gene expression in DFCs or a lack of KV and cilia formation in mutants; *n*, number of embryos scored as wild-type/total number of embryos examined from a heterozygous cross (~25% are mutant); *N*=number of mutant embryos analyzed (selected from wild-type sibs).

*RNA is expressed, but protein is not (Shulte-Merker et al., 1994).

†KV forms in most *flh* mutants (Melby et al.., 1996).

nd: not determined.

class I mutants *ntl* and *floating head* (*flh*) have defects in notochord formation and bilateral expression of asymmetry markers; class II mutants *spadetail* (*spt*) and *casanova* (*cas*) have randomized and discordant expression of laterality markers; class III mutant *cyclops* (*cyc*) lacks asymmetric expression of *lft1* in the diencephalon but has normal expression of other asymmetry markers in the heart and gut. Class IV mutants *one-eyed pinhead* (*oep*) and *schmalspur* (*sur*) fail to asymmetrically express *lft1*, *lft2* or *pitx2* in the diencephalon, heart and gut, probably owing to a direct disruption of the Nodal signaling pathway in responding cells (Gritsman et al., 1999; Pogoda et al., 2000).

DFCs were observed by DIC microscopy from 60% to 80% epiboly, and usually comprised 15 to 27 cells in wild-type embryos. DFCs have strong endocytic activity from the dome stage to 70% epiboly that can be assessed by staining with the fluorescent vital dye SYTO-11 (Cooper and D'Amico, 1996). Each of the laterality mutants, with the exception of *cas*, had DFCs that were endocytically active and had normal *ntl* expression (Table 3). In our study, *cas* mutants had DFCs, but they were fewer (average 10.5 cells/embryo), flatter, more disperse and did not take up SYTO-11. This somewhat concurs with a previous report (Alexander et al., 1999) that *cas* mutants lack DFCs, and indicates that *cas*, a Sox-related transcription factor, is required for DFC formation and endocytic activity. With the exception of *cas*, the formation of DFCs, their organization and their endocytic activity during gastrulation do not appear to be correlated with later laterality defects in the mutants examined.

To identify genetic pathway(s) upstream of *lrdr1*, laterality mutants were examined for *lrdr1* expression in DFCs during gastrulation. Strikingly, *ntl* mutant embryos, which lack the Ntl T-box transcription factor (homologous to mouse brachyury), either failed to express *lrdr1* in DFCs or had only a few DFCs

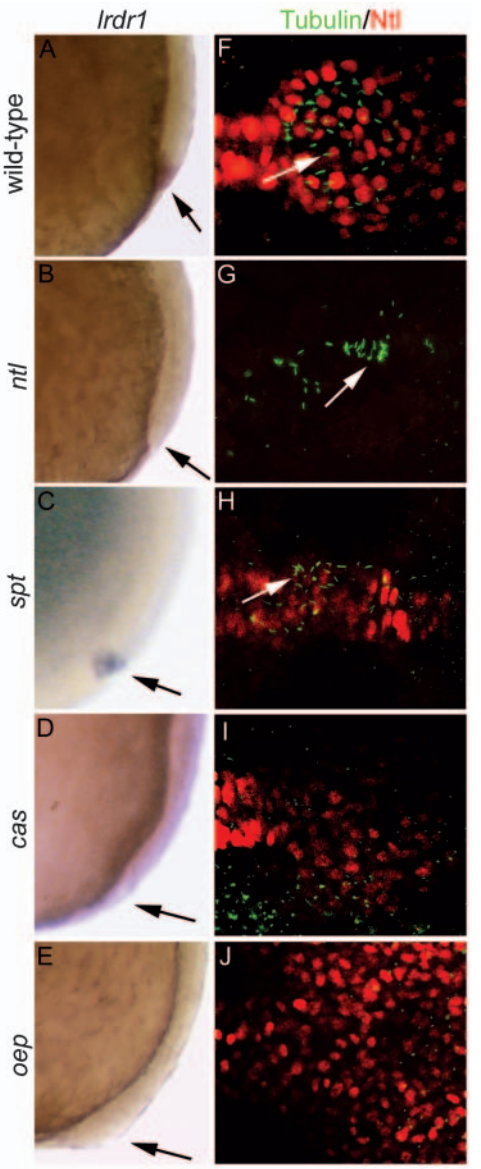

Fig. 5. *ntl* and the Nodal signaling pathway regulate *lrdr1* expression, and, with other genes, control morphogenesis of Kupffer's vesicle. Wild-type (A,F) and mutant *ntl*^{b195}(B,G), *spt*^{b104}(C,H), *cas*^{ta56} (D,I) and *oep*^{m134} (E,J) embryos were examined for *lrdr1* mRNA expression, cilia formation and KV organization. (A-E) *lrdr1* expression at 80-90% epiboly. Lateral views, dorsal towards the right, anterior upwards; arrows indicate DFCs. (F-J) Immunofluorescence analysis of cilia and KV morphogenesis using anti-acetylated Tubulin antibodies (cilia, green) and anti-Ntl antibodies (KV, red) at 6-10 SS. Dorsal views with anterior towards the left. Arrows indicate cilia.

that weakly expressed *lrdr1* (Fig. 5B and Table 3). DFCs in *ntl* mutants appeared normal, expressed the Nodal family member *sqt* and *ntl* RNA, and were able to uptake SYTO-11 (Table 3). Another T-box transcription factor gene, *spt*, is expressed in DFCs (data not shown) but is not required for *lrdr1* expression, as *spt* mutants display normal *lrdr1* expression patterns (Fig. 5C and Table 3). *cas* mutants also lacked *lrdr1* expression (Fig. 5D and Table 3), probably owing to aberrant DFC formation. These results indicate that Ntl, but not the closely related T-box transcription factor Spt, is upstream of *lrdr1*. This is the first identification of a transcription factor upstream of *dynein* expression in ciliated node-like cells in any vertebrate embryo.

Analyses of zebrafish cell-signaling mutants revealed that the Nodal signaling pathway is also upstream of *lrdr1* expression. DFCs in zygotic *oep* mutants were properly formed, endocytically active and expressed *ntl*, but failed to express *lrdr1* (Fig. 5E and Table 3). Oep is an EGF-CFC co-receptor that is essential for the reception of Nodal signaling (Gritsman et al., 1999). Consistent with these results, *lrdr1* mRNA was not detected in maternal-zygotic *sur* (mz*sur*) mutants (n=0/25) that lack a forkhead transcription factor (Foxa1) thought to directly respond to Nodal signaling (Pogoda et al., 2000). Zygotic cyc^{tf219} mutants had normal *ntl* expression (n=56/56 embryos from heterozygote crosses) and *lrdr1* expression (n=263/264). Cyclops is a distinct Nodal-related ligand (Rebagliati et al., 1998; Sampath et al., 1998). Together, this mutant analysis indicates that Nodal signaling through *oep* and *sur*, but not the zygotically expressed Cyclops member of the Nodal family, is upstream of *lrdr1*expression. As discussed below, these results identify two genetic pathways that are required, either directly or indirectly, for *lrdr1* expression in the DFCs: the *ntl* pathway and the Nodal signaling pathway.

Last, we screened laterality mutants for KV organogenesis and ciliogenesis within KV. *ntl* mutants (identified by a lack of Ntl immunostaining) formed patches of cells with anti-Tubulin labeled cilia, but these embryos failed to develop a normal KV (Fig. 5G; Table 3). In *spt* mutants, *lrdr1* expression was normal and tubulin immunostaining detected cilia, but KV was disorganized (Fig. 5H and Table 3). *cas* and *oep* mutants showed an absence of both cilia and KV (Fig. 5I,J; Table 3). Notably, *ntl*, *spt*, *oep* and *cas* mutants all lead to the same endpoint of defective KV morphogenesis, but block distinct steps leading to a functional KV and affect downstream LR gene expression in dramatically different manners.

Discussion

Cilia located on the ventral surface of the mouse node are thought to initiate LR development by generating a nodal flow that establishes asymmetric gene expression. Previous work has suggested that a similar ciliary-based mechanism within the embryonic node/organizer/shield in chick, *Xenopus* and zebrafish embryos may function to generate LR asymmetry in other vertebrate species, but no direct functional analysis has been reported. In zebrafish, dorsal forerunner cells (DFCs) and their progeny in Kupffer's vesicle (KV) express *lrdr1*, a dynein gene family member, and KV cells are ciliated (Essner et al., 2002), similar to KV cells in another teleost fish, *Fundulus heteroclitus* (Brummett and Dumont, 1978). Another component of cilia, Inversin, has been found in several vertebrates and has been implicated in LR heart orientation in zebrafish (Morgan et al., 2002b; Otto et al., 2003). Furthermore, *pkd2*, which encodes a component of a cation channel (Hanaoka et al., 2000) that localizes to cilia in mouse cells (Yoder et al., 2002), has been shown to function during zebrafish kidney development (Sun et al., 2004) and LR determination (data not shown). However, four observations leave open the possibility that nodal cilia are not the loci of activity for LR development in any vertebrate. First, genes implicated in cilia formation or function and LR development are expressed ubiquitously in early development, for example, *lrd* (*iv*) in mice (Supp et al., 1999), *lrdr1* in zebrafish (this report) and inversin (*Invs*) in mice (Mochizuki et al., 1998; Morgan et al., 1998) and zebrafish (data not shown). Genes implicated in mouse nodal cilia function have not been knocked out exclusively in the mouse node, and it is clear from the pleiotropic mutant phenotypes that some of these genes have other roles in development that, when perturbed, could lead to defects in LR development (reviewed by Wagner and Yost, 2000). Second, Inversin protein is found not only in cilia but in other intracellular locations (Eley et al., 2004; Morgan et al., 2002a; Nurnberger et al., 2002; Nurnberger et al., 2004), suggesting it has non-ciliary functions. Third, cilia are found in other embryonic tissues such as the embryonic midline (Sulik et al., 1994), which has been implicated in LR development in frogs, zebrafish and mice (Danos and Yost, 1995; Danos and Yost, 1996; Meno et al., 1998), suggesting functions ascribed to cilia genes in LR development might occur in non-node cells. Fourth, motor molecules have been implicated in earlier steps in LR patterning in *Xenopus* (Levin, 2003).

Here, using zebrafish embryos, we provide the first evidence that ciliated cells function during LR development in a non-murine embryo. Laser ablation of DFCs, which perturbs KV morphogenesis, and surgical disruption of KV directly show that DFC/KV cells play an essential role in zebrafish LR patterning. We also show that cilia in KV are motile and generate a directional fluid flow that is severely impaired by MO knockdown of *lrdr1*, which consequently alters LR development. Finally, analysis of LR mutations in zebrafish has revealed novel roles for both the *ntl* and *Nodal* pathways in the regulation, either directly or indirectly, of *lrdr1* expression for the regulation of LR development.

Using a recently developed technique that targets MO to DFC/KV cells (Amack and Yost, 2004), we have found that *lrdr1* expression in DFC/KV cells is required for normal LR development. MO injected into the yolk cell at mid-blastula stages often enter DFCs, and not other cells, probably via cytoplasmic bridges first characterized by Cooper and D'Amico (1996) by loading fluorescent dextran into the yolk between the 1000-cell to oblong stages. Dextran accumulated in at least some DFCs in ~60% of these embryos and was also often found in some non-DFC marginal cells, indicating that both DFCs and other margin cells are potentially in cytoplasmic confluence with the yolk. We have observed similar results injecting fluorescent-tagged MO into the yolk cell at mid-blastula stages, including a high degree of embryo-to-embryo variability. Fluorescence microscopy was used to select embryos in which MO have loaded into DFCs but not other embryonic cells. It is possible that small amounts of MO, below detection by fluorescent microscopy, accumulate in cells other than DFCs. To test this, we targeted DFCs with MO

against another gene that is required for normal LR development, *lft1*, which is not expressed DFCs, but in cells neighboring DFCs (Fig. 1B-D). Eighty-two percent of DFC^{lft1MO} embryos showed normal asymmetric *lft2* expression (Table 1), indicating MO injected into the yolk at mid-blastula stages do not affect non-DFC cells. In a separate control for DFC^{MO} experiments, embryos injected with *lrdr1* MO into the underlying yolk syncitial layer (YSL) cells at stages when bridges between the YSL and DFCs have closed (dome stage to 30% epiboly) have normal LR development. Although this does not exclude a possible role for the YSL in LR development, it indicates that *lrdr1* (this study) and *ntl* (Amack and Yost, 2004) do not function in YSL during LR patterning. Taken together, the results from three approaches – DFC ablation, KV surgical disruption and *lrdr1* knockdown in DFC/KV cells – demonstrate that the ciliated KV is an embryonic organ of asymmetry that is required for the earliest known step in the generation of LR asymmetry in zebrafish.

Multiple pathways for Kupffer's Vesicle development and establishment of LR asymmetry

Our analysis of KV formation and function in zebrafish mutants provides a template for reconsidering distinct phenotypes seen in mouse and human laterality syndromes (Bisgrove et al., 2003). Based on our results, we propose five distinct steps in KV that precede the earliest known asymmetric gene expression patterns in zebrafish (Fig. 6). In the first step, DFCs are induced during the blastula period. As previously reported (Alexander et al., 1999) and shown here, *cas* mutant embryos, which are deficient for a novel Sox-related gene and lack all endoderm, also lack normal DFCs. The few DFCs present in *cas* mutants are misshapen and defective in: endocytosis; *lrdr1*, *ntl* and *sqt* expression; ciliogenesis; and formation of KV. As *cas* was originally isolated as a cDNA responsive to Nodal signaling (Dickmeis et al., 2001) and two Nodal-related ligands, *sqt* and *cyc*, are expressed in close proximity to DFCs (Rebagliati et al., 1998), the Nodal pathway is strongly implicated in the induction of the DFCs. However, as *cyc*^{tf219} mutants form DFCs that are SYTO-11 positive and express *lrdr1*, it is likely that other members of the Nodal family, perhaps maternally stored, are important for the formation of DFCs.

The second step in the KV pathway is the activation of *lrdr1* expression in DFCs at the end of gastrulation. DFCs in mutants that lack *oep*, a Nodal signaling co-receptor, or mz*sur*, a *foxa1* transcription factor in the Nodal response pathway, fail to express *lrdr1*. In addition to Nodal signaling, *ntl* mutant embryos fail to express *lrdr1* in the DFCs, suggesting that Ntl transcription factor is upstream of *lrdr1*. As *ntl* mutants have a normal number of DFCs that stain with SYTO-11, express *ntl* mutant RNA and *sqt* RNA, and form cilia (Table 3), it is unlikely that the absence of *lrdr1* expression in *ntl* mutants is due to non-specific changes in DFC determination. In some cases, *ntl* can be induced by the Activin/Nodal pathway (Bisgrove et al., 1999; Toyama et al., 1995); one could propose that Nodal signaling is upstream of *ntl*, which is then upstream of *lrdr1*. However, Ntl protein is expressed in *oep* mutants that lack *lrdr1* expression, although there might be a subtle and undetectable decrease in Ntl in *oep* mutants. In addition, DFCs in *ntl* and *oep* mutants differ in *sqt* expression and cilia formation. Together, this suggests that the *ntl*-dependent induction of *lrdr1* is a pathway parallel to the Nodal pathway. Obviously, mutant analysis indicates that *lrdr1* expression is dependent on *ntl* and components of the Nodal pathway, but does not distinguish whether this dependence is direct or indirect. Clearly, both of these genetic pathways have other functions in KV development beyond regulation of *lrdr1* expression (Fig. 6), as *lrdr1* morphants do not display defects in KV organogenesis and cilia formation seen in *ntl* and *oep* mutants. Conversely, although knockdown of *lrdr1* disrupts directional fluid flow in the KV, one cannot exclude other roles for *lrdr1* within DFC/KV cells for LR development.

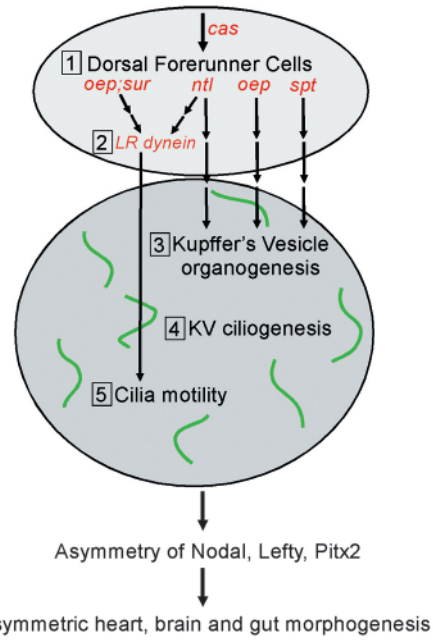

Fig. 6. Multiple genetic pathways control the formation and function of Kupffer's vesicle to direct LR development. We propose five steps (1-5) that are required to set up normal asymmetric expression patterns of Nodal, Lefty and Pitx2 gene family members and subsequent morphological asymmetry of the heart, brain and gut in the zebrafish embryo. First, DFCs are specified during the blastula period. Probably among a number of yet unidentified factors, *cas* is required for proper DFC formation. Second, the *ntl* and *oep* (Nodal signaling) pathways control the expression of Left-Right dynein (*lrdr1*), a ciliary motor protein, in DFCs. Third, DFCs organize to form KV during early somitogenesis. *ntl* and *oep* are also essential for this step. By contrast, *spt* is required for KV organogenesis but not for *lrdr1* expression in DFCs. Fourth, cilia assemble on cells lining the fluid-filled lumen of KV. Fifth, KV cilia become motile, which is dependent on left-right dynein, and generate a directional flow of fluid inside KV. We suggest that fluid flow inside KV, a transient embryonic organ of asymmetry, initiates asymmetric gene expression in lateral tissue that leads to normal LR development.

In the third step, DFCs organize to form KV at the completion of gastrulation. This process involves ingression into the forming tailbud and formation of an epithelial sheet at the base of the notochord. KV formation is dependent on Nodal signaling components (exemplified by *oep*) and Ntl, as well as on additional genes that are not required for *lrdr1* expression, including the T-box transcription factor Spt. Using the DFC^{MO} technique, KV organogenesis was found to be cell-autonomously dependent on *ntl* (Amack and Yost, 2004). It is

not yet known whether defects in KV development described here (Table 3) are cell autonomous for *spt* and components of the Nodal pathway.

In the fourth step, cilia form on KV cells and project into the lumen. Surprisingly, cilia formation can be uncoupled from the normally coincident formation of KV in step 3, as *spt* and *ntl* mutants do not form an organized KV but form cilia (Fig. 5G,H; Table 3). In agreement with observations in *Dnahc11/Dnahc11* mice (Supp et al., 1999), cilia formation in zebrafish does not appear to be dependent on *lrdr1*, as cilia are found in *ntl* mutants that lack normal *lrdr1* expression (Fig. 5G) and in *lrdr1* morphant embryos (Fig. 4H). In the fifth step, cilia motility and fluid flow in KV is dependent on *lrdr1*, which determines normal asymmetric gene expression patterns in lateral tissues.

This mutant analysis points out that perturbation of one or combinations of the five steps in KV function outlined above results in altered LR development in the brain, heart and gut. Of the characteristics we examined, defects in KV organogenesis alone (e.g. *spt*), KV organogenesis plus *lrdr1* expression (e.g. *ntl*), KV ciliogenesis, organogenesis and *lrd1* expression (e.g. *oep*), or all of the above plus DFC formation (e.g. *cas*) results in LR abnormalities. Interestingly, each of the mutants has distinct expression patterns of downstream laterality markers (Bisgrove et al., 2000). Although it might be tempting to speculate that defects in the distinct KV steps outlined above result in distinct laterality phenotypes in the rest of the embryo, it is important to note that the genes involved are expressed in other cells besides DFC/KV cells, and such a conclusion can not be made until the gene of interest is knocked down specifically in DFC/KV cells. For example, DFC^{MO} knockdown of *ntl* has a laterality phenotype that is distinct from bilateral expression patterns seen in *ntl* mutants and whole-embryo *ntl* morphants, indicating that *ntl* has distinct roles in DFC/KV and in midline cells for LR development (Amack and Yost, 2004). Our surgical disruptions of KV indicate that KV is no longer needed for LR development by 10 SS, but do not exclude the possibility that different LR signals come from the DFCs or the KV at earlier stages in DFC/KV development.

How does KV fluid flow control lateral asymmetric gene expression?

Several models have been proposed to explain how cilia movement and fluid flow influences LR development, and how this information is transmitted to lateral plate mesoderm to initiate asymmetric expression of Nodal, Lefty and Pitx2 (for review (Mercola, 2003; Raya and Belmonte, 2004)). Flow has been proposed to influence the localization of a signaling molecule (Okada et al., 1999) or asymmetric activation of mechanosensory cilia and intracellular Ca^{2+} (McGrath et al., 2003) in mice. In chick, nodal cilia are present (Essner et al., 2002). Although motility and nodal flow have not been reported, extracellular Ca^{2+} has been proposed to activate lateral asymmetric nodal expression via a Notch-dependent pathway (Raya et al., 2004). Here, we show in zebrafish that *lrdr1*-dependent asymmetric fluid flow in KV probably results in asymmetric gene expression that sweeps from the tail to the head of the developing embryo. However, the mechanisms by which counterclockwise flow in KV is translated to molecular asymmetries near KV are not known.

In zebrafish, *charon*, an inhibitor of nodal signaling, is expressed in the tailbud at 2-3 SS during the formation of KV and then symmetrically adjacent to KV until the 14 SS (Hashimoto et al., 2004). Southpaw (*spaw*), a member of the nodal family, is bilaterally expressed immediately adjacent to *charon* (Hashimoto et al., 2004; Long et al., 2003). Morpholino knockdown of *charon* results in bilateral expression of *spaw* and other asymmetric markers in lateral plate mesoderm (*cyc*, *lefty* and *pitx2*). Conversely, knockdown of *spaw* results in absence of downstream asymmetric markers. It is not known how the symmetric expression patterns of *charon* and *spaw* control subsequent asymmetric expression of *spaw* and other downstream genes. However, the bilateral *spaw* and *charon* expression near KV during the period that we have shown KV is important in LR development suggests that information derived from the *lrdr1*-dependent asymmetric fluid flow might influence the balance or interactions of *spaw* and its antagonist *charon* in adjacent cells.

There is elegance in the frugality of using the same signaling pathway at multiple stages in LR development. The T-box transcription factor Ntl independently drives *lrdr1* expression and KV morphogenesis (Fig. 6) and midline formation in mesoderm cells, both of which are necessary for distinct aspects of normal asymmetric gene expression in lateral plate (Amack and Yost, 2004). Similarly, the Nodal signaling pathway is required for the induction of *lrdr1* gene expression in DFCs in order to drive motile cilia in Kupffer's vesicle, and ciliated KV is necessary for driving normal LR asymmetric expression of components of the Nodal signaling pathway in lateral mesoderm. This novel aspect of the Nodal pathway, upstream of *lrdr1* function, suggests that analyses that have implicated the Nodal pathway in LR development in mice, chick, frog and zebrafish should be re-investigated for proximal defects in the formation and function of ciliated cells.

Conservation of a ciliary-based mechanism for LR development

Several lines of evidence presented here indicate that KV cilia in zebrafish are required in LR development and are analogous to cilia located on the ventral mouse node. However, it is not known whether the generation of a flow in KV is the first symmetry breaking event in zebrafish. Certainly, the appearance of motile cilia in the KV, and the developmental period during which DFC/KV manipulations can alter LR development, precedes the appearance of asymmetric gene expression of *spaw*, *cyc*, *lft1* and *lft2* in lateral tissues. As such, it is the earliest known event in zebrafish LR development. However, recent evidence from frog embryos suggests that asymmetries are generated long before the appearance of ciliated cells (Kramer et al., 2002; Kramer and Yost, 2002; Levin et al., 2002). It is not yet known whether these mechanisms are amphibian specific, and future work will be focused on investigating potential connections between early molecular asymmetries and nodal flow. In chick, *lrdr* expression and cilia are found at stage HH4 (Essner et al., 2002), but more detailed expression analysis, cilia motility and fluid flow have not been reported, making it difficult to know whether early molecular asymmetries (Levin et al., 1995; Stern et al., 1995) precede a role for cilia. The results presented here demonstrate the importance of cilia in Kupffer's vesicle, a transient embryonic organ of asymmetry, for the establishment

of left-right asymmetry in the gut, heart and brain in zebrafish. These data provide the first direct functional evidence of a ciliary-based mechanism operating in a non-murine vertebrate embryo during LR patterning.

We thank M. Brueckner for sharing mouse LRD sequences during our cloning of *lrdr1*, and B. Bisgrove, W. Branford and M. L. Condic for comments on the manuscript. M. Yoshigi and T. Cooke (from A. G. Heinze) provided technical assistance in imaging cilia in live embryos. This work was supported in part by grants from NIHLB and the Huntsman Cancer Foundation to H.J.Y. and an NRSA fellowship to J.D.A.

Supplementary material

Supplementary material for this article is available at
http://dev.biologists.org/cgi/content/full/132/6/1247/DC1

References

Alexander, J., Rothenberg, M., Henry, G. L. and Stainier, D. Y. (1999). casanova plays an early and essential role in endoderm formation in zebrafish. *Dev. Biol.* **215**, 343-357.

Amack, J. D. and Yost, H. J. (2004). The T box transcription factor no tail in ciliated cells controls zebrafish left-right asymmetry. *Curr. Biol.* **14**, 685-690.

Bisgrove, B. W., Essner, J. J. and Yost, H. J. (1999). Regulation of midline development by antagonism of lefty and nodal signaling. *Development* **126**, 3253-3262.

Bisgrove, B. W., Essner, J. J. and Yost, H. J. (2000). Multiple pathways in the midline regulate concordant brain, heart and gut left-right asymmetry. *Development* **127**, 3567-3579.

Bisgrove, B. W., Morelli, S. H. and Yost, H. J. (2003). Genetics of human laterality disorders: insights from vertebrate model systems. *Annu. Rev. Genomics Hum. Genet.* **4**, 1-32.

Brown, N. A., Hoyle, C. I., McCarthy, A. and Wolpert, L. (1989). The development of asymmetry: the sidedness of drug-induced limb abnormalities is reversed in situs inversus mice. *Development* **107**, 637-642.

Brummett, A. R. and Dumont, J. N. (1978). Kupffer's vesicle in Fundulus heteroclitus: a scanning and transmission electron microscope study. *Tiss. Cell* **10**, 11-22.

Chen, J. N., van Eeden, F. J., Warren, K. S., Chin, A., Nusslein-Volhard, C., Haffter, P. and Fishman, M. C. (1997). Left-right pattern of cardiac BMP4 may drive asymmetry of the heart in zebrafish. *Development* **124**, 4373-4382.

Chin, A. J., Tsang, M. and Weinberg, E. S. (2000). Heart and gut chiralities are controlled independently from initial heart position in the developing zebrafish. *Dev. Biol.* **227**, 403-421.

Concha, M. L., Burdine, R. D., Russell, C., Schier, A. F. and Wilson, S. W. (2000). A nodal signaling pathway regulates the laterality of neuroanatomical asymmetries in the zebrafish forebrain. *Neuron* **28**, 399-409.

Cooper, M. S. and D'Amico, L. A. (1996). A cluster of noninvoluting endocytic cells at the margin of the zebrafish blastoderm marks the site of embryonic shield formation. *Dev. Biol.* **180**, 184-198.

D'Amico, L. A. and Cooper, M. S. (1997). Spatially distinct domains of cell behavior in the zebrafish organizer region. *Biochem. Cell Biol.* **75**, 563-577.

D'Amico, L. A. and Cooper, M. S. (2001). Morphogenetic domains in the yolk syncytial layer of axiating zebrafish embryos. *Dev. Dyn.* **222**, 611-624.

Danos, M. C. and Yost, H. J. (1995). Linkage of cardiac left-right asymmetry and dorsal-anterior development in Xenopus. *Development* **121**, 1467-1474.

Danos, M. C. and Yost, H. J. (1996). Role of notochord in specification of cardiac left-right orientation in zebrafish and Xenopus. *Dev. Biol.* **177**, 96-103.

Dickmeis, T., Mourrain, P., Saint-Etienne, L., Fischer, N., Aanstad, P., Clark, M., Strahle, U. and Rosa, F. (2001). A crucial component of the endoderm formation pathway, CASANOVA, is encoded by a novel sox-related gene. *Genes Dev.* **15**, 1487-1492.

Draper, B. W., Morcos, P. A. and Kimmel, C. B. (2001). Inhibition of zebrafish fgf8 pre-mRNA splicing with morpholino oligos: a quantifiable method for gene knockdown. *Genesis* **30**, 154-156.

Eley, L., Turnpenny, L., Yates, L. M., Craighead, A. S., Morgan, D., Whistler, C., Goodship, J. A. and Strachan, T. (2004). A perspective on inversin. *Cell Biol. Int.* **28**, 119-124.

Essner, J. J., Branford, W. W., Zhang, J. and Yost, H. J. (2000). Mesendoderm and left-right brain, heart and gut development are differentially regulated by pitx2 isoforms. *Development* **127**, 1081-1093.

Essner, J. J., Vogan, K. J., Wagner, M. K., Tabin, C. J., Yost, H. J. and Brueckner, M. (2002). Conserved function for embryonic nodal cilia. *Nature* **418**, 37-38.

Feldman, B., Concha, M. L., Saude, L., Parsons, M. J., Adams, R. J., Wilson, S. W. and Stemple, D. L. (2002). Lefty antagonism of Squint is essential for normal gastrulation. *Curr. Biol.* **12**, 2129-2135.

Gamse, J. T., Thisse, C., Thisse, B. and Halpern, M. E. (2003). The parapineal mediates left-right asymmetry in the zebrafish diencephalon. *Development* **130**, 1059-1068.

Gritsman, K., Zhang, J., Cheng, S., Heckscher, E., Talbot, W. S. and Schier, A. F. (1999). The EGF-CFC protein one-eyed pinhead is essential for nodal signaling. *Cell* **97**, 121-132.

Hanaoka, K., Qian, F., Boletta, A., Bhunia, A. K., Piontek, K., Tsiokas, L., Sukhatme, V. P., Guggino, W. B. and Germino, G. G. (2000). Co-assembly of polycystin-1 and -2 produces unique cation-permeable currents. *Nature* **408**, 990-994.

Hashimoto, H., Rebagliati, M., Ahmad, N., Muraoka, O., Kurokawa, T., Hibi, M. and Suzuki, T. (2004). The Cerberus/Dan-family protein Charon is a negative regulator of Nodal signaling during left-right patterning in zebrafish. *Development* **131**, 1741-1753.

Kimmel, C. B. and Law, R. D. (1985). Cell lineage of zebrafish blastomeres. II. Formation of the yolk syncytial layer. *Dev. Biol.* **108**, 86-93.

Kramer, K. L. and Yost, H. J. (2002). Ectodermal syndecan-2 mediates left-right axis formation in migrating mesoderm as a cell-nonautonomous Vg1 cofactor. *Dev. Cell* **2**, 115-124.

Kramer, K. L., Barnette, J. E. and Yost, H. J. (2002). PKCgamma regulates syndecan-2 inside-out signaling during xenopus left-right development. *Cell* **111**, 981-990.

Krauss, S., Concordet, J. P. and Ingham, P. W. (1993). A functionally conserved homolog of the Drosophila segment polarity gene hh is expressed in tissues with polarizing activity in zebrafish embryos. *Cell* **75**, 1431-1444.

Kupffer, C. (1868). Beobachtungea uber die Entwicklung der Knochenfische. *Arch. Mikrob. Anat.* **4**, 209-272.

Levin, M. (2003). Motor protein control of ion flux is an early step in embryonic left-right asymmetry. *BioEssays* **25**, 1002-1010.

Levin, M., Johnson, R. L., Stern, C. D., Kuehn, M. and Tabin, C. (1995). A molecular pathway determining left-right asymmetry in chick embryogenesis. *Cell* **82**, 803-814.

Levin, M., Thorlin, T., Robinson, K. R., Nogi, T. and Mercola, M. (2002). Asymmetries in H+/K+-ATPase and cell membrane potentials comprise a very early step in left-right patterning. *Cell* **111**, 77-89.

Lohr, J. L., Danos, M. C. and Yost, H. J. (1997). Left-right asymmetry of a nodal-related gene is regulated by dorsoanterior midline structures during Xenopus development. *Development* **124**, 1465-1472.

Long, S., Ahmad, N. and Rebagliati, M. (2003). The zebrafish nodal-related gene southpaw is required for visceral and diencephalic left-right asymmetry. *Development* **130**, 2303-2316.

Marszalek, J. R., Ruiz-Lozano, P., Roberts, E., Chien, K. R. and Goldstein, L. S. (1999). Situs inversus and embryonic ciliary morphogenesis defects in mouse mutants lacking the KIF3A subunit of kinesin-II. *Proc. Natl. Acad. Sci. USA* **96**, 5043-5048.

McGrath, J., Somlo, S., Makova, S., Tian, X. and Brueckner, M. (2003). Two populations of node monocilia initiate left-right asymmetry in the mouse. *Cell* **114**, 61-73.

Melby, A. E., Warga, R. M. and Kimmel, C. B. (1996). Specification of cell fates at the dorsal margin of the zebrafish gastrula. *Development* **122**, 2225-2237.

Meno, C., Shimono, A., Saijoh, Y., Yashiro, K., Mochida, K., Ohishi, S., Noji, S., Kondoh, H. and Hamada, H. (1998). lefty-1 is required for left-right determination as a regulator of lefty-2 and nodal. *Cell* **94**, 287-297.

Mercola, M. (2003). Left-right asymmetry: nodal points. *J. Cell Sci.* **116**, 3251-3257.

Mochizuki, T., Saijoh, Y., Tsuchiya, K., Shirayoshi, Y., Takai, S., Taya, C., Yonekawa, H., Yamada, K., Nihei, H., Nakatsuji, N. et al. (1998). Cloning of inv, a gene that controls left/right asymmetry and kidney development. *Nature* **395**, 177-181.

Morgan, D., Eley, L., Sayer, J., Strachan, T., Yates, L. M., Craighead, A. S. and Goodship, J. A. (2002a). Expression analyses and interaction with the anaphase promoting complex protein Apc2 suggest a role for inversin

in primary cilia and involvement in the cell cycle. *Hum. Mol. Genet.* **11**, 3345-3350.

Morgan, D., Goodship, J., Essner, J. J., Vogan, K. J., Turnpenny, L., Yost, H. J., Tabin, C. J. and Strachan, T. (2002b). The left-right determinant inversin has highly conserved ankyrin repeat and IQ domains and interacts with calmodulin. *Hum. Genet.* **110**, 377-384.

Morgan, D., Turnpenny, L., Goodship, J., Dai, W., Majumder, K., Matthews, L., Gardner, A., Schuster, G., Vien, L., Harrison, W. et al. (1998). Inversin, a novel gene in the vertebrate left-right axis pathway, is partially deleted in the inv mouse. *Nat. Genet.* **20**, 149-156.

Murcia, N. S., Richards, W. G., Yoder, B. K., Mucenski, M. L., Dunlap, J. R. and Woychik, R. P. (2000). The Oak Ridge Polycystic Kidney (orpk) disease gene is required for left-right axis determination. *Development* **127**, 2347-2355.

Nasevicius, A. and Ekker, S. C. (2000). Effective targeted gene 'knockdown' in zebrafish. *Nat. Genet.* **26**, 216-220.

Nonaka, S., Tanaka, Y., Okada, Y., Takeda, S., Harada, A., Kanai, Y., Kido, M. and Hirokawa, N. (1998). Randomization of left-right asymmetry due to loss of nodal cilia generating leftward flow of extraembryonic fluid in mice lacking KIF3B motor protein. *Cell* **95**, 829-837.

Nonaka, S., Shiratori, H., Saijoh, Y. and Hamada, H. (2002). Determination of left-right patterning of the mouse embryo by artificial nodal flow. *Nature* **418**, 96-99.

Nurnberger, J., Bacallao, R. L. and Phillips, C. L. (2002). Inversin forms a complex with catenins and N-cadherin in polarized epithelial cells. *Mol. Biol. Cell* **13**, 3096-3106.

Nurnberger, J., Kribben, A., Saez, A. O., Heusch, G., Philipp, T. and Phillips, C. L. (2004). The Invs gene encodes a microtubule-associated protein. *J. Am. Soc. Nephrol.* **15**, 1700-1710.

Okada, Y., Nonaka, S., Tanaka, Y., Saijoh, Y., Hamada, H. and Hirokawa, N. (1999). Abnormal nodal flow precedes situs inversus in iv and inv mice. *Mol. Cell* **4**, 459-468.

Otto, E. A., Schermer, B., Obara, T., O'Toole, J. F., Hiller, K. S., Mueller, A. M., Ruf, R. G., Hoefele, J., Beekmann, F., Landau, D. et al. (2003). Mutations in INVS encoding inversin cause nephronophthisis type 2, linking renal cystic disease to the function of primary cilia and left-right axis determination. *Nat. Genet.* **34**, 413-420.

Pogoda, H. M., Solnica-Krezel, L., Driever, W. and Meyer, D. (2000). The zebrafish forkhead transcription factor FoxH1/Fast1 is a modulator of nodal signaling required for organizer formation. *Curr. Biol.* **10**, 1041-1049.

Raya, A. and Belmonte, J. C. (2004). Sequential transfer of left-right information during vertebrate embryo development. *Curr. Opin. Genet. Dev.* **14**, 575-581.

Raya, A., Kawakami, Y., Rodriguez-Esteban, C., Ibanes, M., Rasskin-Gutman, D., Rodriguez-Leon, J., Buscher, D., Feijo, J. A. and Izpisua Belmonte, J. C. (2004). Notch activity acts as a sensor for extracellular calcium during vertebrate left-right determination. *Nature* **427**, 121-128.

Rebagliati, M. R., Toyama, R., Fricke, C., Haffter, P. and Dawid, I. B. (1998). Zebrafish nodal-related genes are implicated in axial patterning and establishing left-right asymmetry. *Dev. Biol.* **199**, 261-272.

Sampath, K., Rubinstein, A. L., Cheng, A. M., Liang, J. O., Fekany, K., Solnica-Krezel, L., Korzh, V., Halpern, M. E. and Wright, C. V. (1998). Induction of the zebrafish ventral brain and floorplate requires cyclops/nodal signalling. *Nature* **395**, 185-189.

Schulte-Merker, S., Ho, R. K., Herrmann, B. G. and Nusslein-Volhard, C. (1992). The protein product of the zebrafish homologue of the mouse T gene is expressed in nuclei of the germ ring and the notochord of the early embryo. *Development* **116**, 1021-1032.

Schulte-Merker, S., van Eeden, F. J., Halpern, M. E., Kimmel, C. B. and Nusslein-Volhard, C. (1994). no tail (ntl) is the zebrafish homologue of the mouse T (Brachyury) gene. *Development* **120**, 1009-1015.

Stern, C. D., Yu, R. T., Kakizuka, A., Kintner, C. R., Mathews, L. S., Vale, W. W., Evans, R. M. and Umesono, K. (1995). Activin and its receptors during gastrulation and the later phases of mesoderm development in the chick embryo. *Dev. Biol.* **172**, 192-205.

Sulik, K., Dehart, D. B., Iangaki, T., Carson, J. L., Vrablic, T., Gesteland, K. and Schoenwolf, G. C. (1994). Morphogenesis of the murine node and notochordal plate. *Dev. Dyn.* **201**, 260-278.

Sun, Z., Amsterdam, A., Pazour, G. J., Cole, D. G., Miller, M. S. and Hopkins, N. (2004). A genetic screen in zebrafish identifies cilia genes as a principal cause of cystic kidney. *Development* **131**, 4085-4093.

Supp, D. M., Witte, D. P., Potter, S. S. and Brueckner, M. (1997). Mutation of an axonemal dynein affects left-right asymmetry in inversus viscerum mice. *Nature* **389**, 963-966.

Supp, D. M., Brueckner, M., Kuehn, M. R., Witte, D. P., Lowe, L. A., McGrath, J., Corrales, J. and Potter, S. S. (1999). Targeted deletion of the ATP binding domain of left-right dynein confirms its role in specifying development of left-right asymmetries. *Development* **126**, 5495-5504.

Tabin, C. J. and Vogan, K. J. (2003). A two-cilia model for vertebrate left-right axis specification. *Genes Dev.* **17**, 1-6.

Takeda, S., Yonekawa, Y., Tanaka, Y., Okada, Y., Nonaka, S. and Hirokawa, N. (1999). Left-right asymmetry and kinesin superfamily protein KIF3A: new insights in determination of laterality and mesoderm induction by kif3A-/- mice analysis. *J. Cell Biol.* **145**, 825-836.

Thisse, C. and Thisse, B. (1999). Antivin, a novel and divergent member of the TGFbeta superfamily, negatively regulates mesoderm induction. *Development* **126**, 229-240.

Toyama, R., O'Connell, M. L., Wright, C. V., Kuehn, M. R. and Dawid, I. B. (1995). Nodal induces ectopic goosecoid and lim1 expression and axis duplication in zebrafish. *Development* **121**, 383-391.

Wagner, M. K. and Yost, H. J. (2000). Left-right development: the roles of nodal cilia. *Curr. Biol.* **10**, R149-R151.

Warga, R. M. and Stainier, D. Y. (2002). The guts of endoderm formation. *Results Probl. Cell Differ.* **40**, 28-47.

Westerfield, M. (1995). *The Zebrafish Book*. Eugene, OR: University of Oregon Press.

Yamamoto, M., Mine, N., Mochida, K., Sakai, Y., Saijoh, Y., Meno, C. and Hamada, H. (2003). Nodal signaling induces the midline barrier by activating Nodal expression in the lateral plate. *Development* **130**, 1795-1804.

Yoder, B. K., Hou, X. and Guay-Woodford, L. M. (2002). The polycystic kidney disease proteins, polycystin-1, polycystin-2, polaris, and cystin, are co-localized in renal cilia. *J. Am. Soc. Nephrol.* **13**, 2508-2516.

Yost, H. J. (1999). Diverse initiation in a conserved left-right pathway? *Curr. Opin. Genet. Dev.* **9**, 422-426.

Yost, H. J. (2003). Left-right asymmetry: nodal cilia make and catch a wave. *Curr. Biol.* **13**, R808-R809.